VPS VIBRATIONS IN PHYSICAL SYSTEMS

DOI: 10.21008/j.0860-6897.2023.2.15
Vibrations in Physical Systems, 2023, 34(2), 2023215

Novel energy-absorbing auxetic sandwich panel with detached corrugated aluminium layers

Hasan AL-RIFAIE

Poznan University of Technology, Poznan, Poland

Corresponding author: Hasan AL-RIFAIE, Assistant Professor, email: hasan.al-rifaie@put.poznan.pl

Abstract Sandwich panels have the potential to serve as plastically deforming sacrificial structures that can absorb blast or impact energies. Auxetic sandwich panels with welded or bolted corrugated layers have, as far as the author is aware, had their blast behaviour thoroughly addressed in the literature. Therefore, the objective of this numerical analysis was to create a novel, low-cost, simple-to-build graded sandwich panel with detached corrugated layers that may be employed as a multi-purpose sacrificial protective structure against a wide range of blast threats. The suggested sandwich panel has overall dimensions of 330x330x150mm and is made of six detached aluminium (AL6063-T4) layers enclosed in a steel (Weldox 460E) frame. With different stepwise plate thicknesses of 0.4, 0.8, and 1.2mm for each pair of layers, the six layers all have the same re-entrant auxetic geometry. Utilising the Abaqus/Explicit solver, the numerical analysis was carried out. A wide variety of blast intensities (4, 7, 11, 13, and 16 MPa peak reflected over-pressures) were tested on the suggested auxetic sandwich panel, and the results showed uniform progressive collapse, a superior decrease in reaction forces, and greater energy dissipation compared to comparable non-auxetic topologies. The innovative sandwich panel design has potential uses for both military and civic structures that need to be protected.

Keywords: energy absorbers; auxetic; sandwich panels; damping systems; blast; impact; shock; Abaqus.

1. Introduction

Although it is impossible to completely avoid civilian structures being exposed to blast scenarios, the effects of such incidents can be greatly reduced by modifying architecture, design, or retrofitting methods [1, 2]. Hence, it is crucial to have stronger and more effective protective systems [3–5]. Sandwich panels are commonly employed as sacrificial structures to absorb the energy generated by blasts or impacts. Typically, these panel systems comprise a core structure that is sandwiched between two plates, with the frontal plate dispersing the blast pressure evenly across the core, causing it to deform plastically and thereby dissipate the energy of the blast wave [6]. Cellular cores and corrugated cores are among most implemented types of sandwich panels' core structure [7, 8].

Cellular cores can be made of materials such as metallic foams or 3D printed metamaterials. These highly porous materials possess desirable properties such as being lightweight and having excellent energy absorption capabilities [9–11]. Metallic foams, particularly aluminum foams, are usually used for making cellular cores. These foams can be either open-cell or closed-cell structures. Properties and test data are provided in [12–15]. Both numerical and experimental studies have demonstrated the effectiveness of metallic foams in absorbing blast energy. However, due to irregularities in their microstructure, it can be challenging to optimize foam properties for the applied load. Peroni, et al. [16] state that the primary challenges in designing aluminum foams are the material's anisotropy and the significant density variation. Therefore, optimizing the mechanical properties of aluminum foams for practical applications can be a difficult task. The 3D printed meta-materials are considered alternative options because their geometrical parameters can be adjusted to suit specific applications. Honeycomb structures, for example, are utilized in various protective structures due to their excellent energy absorption and impact resistance properties [17–20]. Analytical [21, 22], numerical [23–25] and experimental [26, 27] studies were done to prove their behaviour and characteristics in absorbing shock energy. Although cellular cores offer superior performance, their production often requires relatively expensive techniques [8]. As a result, the use of cellular cores is often limited to specific areas, such as the aerospace industry, biomedical engineering, and military equipment, where their superior performance justifies their higher cost. However, when it comes to protecting larger areas, such as the façade or elevation of an entire building against blast threats, corrugated cores can provide a more cost-effective option for sandwich panels.

Due to their high longitudinal stretching, shear strengths, and energy absorption qualities, corrugated core sandwich panels have been suggested as an appealing substitute for cellular cores [28–30]. The corrugated layers are created using a folding process [31, 32]. Geometric topologies can range from; but not limited to; triangular, sinusoidal, rectangular, and trapezoidal topologies. Studies have been done so far to predict the blast resistance and energy absorption of corrugated core sandwich panels using analytical, computational, and experimental methods [30, 33]. In a comparative study, Rong, et al. [34] investigated the effect of geometric topologies on the behavior of sandwich panels when subjected to small or high-energy impacts. The study found that rectangular and trapezoidal cores had better energy absorption capabilities compared to other structures. However, the forming process for rectangular cores can be challenging, as the stamping die is difficult to separate from the core during fabrication. Therefore, the study concluded that trapezoidal corrugated cores offer a balanced performance and are an excellent structure for engineering applications [34]. The performance of trapezoidal, triangular, sinusoidal and rectangular layer topologies was compared in [35]. The sandwich panels were subjected to ~16MPa peak reflected over-pressure from 0.5kg of TNT at 0.5m stand-off distance. The findings of the study revealed that the trapezoidal topology exhibited superior performance compared to other topologies. It was able to achieve uniform progressive collapse, had lower reaction force, and demonstrated higher plastic dissipation energy [35].

Based on literature, auxetic topologies demonstrate superior energy dissipation when compared to conventional topologies [36–39]. Auxetic structures can exhibit a negative Poisson's ratio [40], which can occur naturally in some materials or can be engineered through microstructural design. One example of a naturally occurring material with a negative Poisson's ratio is α-cristobalite silicon dioxide, although this is a relatively rare occurrence [41]. Some examples of cellular geometries that exhibit auxetic behavior include double arrowhead, re-entrant, chiral, and rotating rigid units [42–44]. In several articles [45–48] and review studies, auxetic structures and their applications have been thoroughly examined [49–54].

According to the author's knowledge, there have been several studies on the impact and blast behavior of sandwich panels with welded, bolted, or riveted corrugated layers. Although these connections provide structural integrity, they can also reduce the plastic dissipation energy of individual layers by affecting their deformation. Therefore, this paper propose a novel panel configuration consisting of unconnected or detached auxetic corrugated layers enclosed in a steel frame. Reaction forces, peak deformations, and plastic dissipation energy are compared for different blast intensities. The new unconnected/non-welded configuration could simplify the production process and make auxetic sandwich panels more cost-effective.

2. Geometrical and material properties of the proposed sandwich panel

The proposed sandwich panel design comprises of a steel frame encasing six corrugated layers, each with a re-entrant topology, that are not connected/bolted/welded to each other. Figure 1 shows the geometry and dimensions of the proposed sandwich panel and its components. Each layer has a total length of 320 mm, extrusion depth of 320 mm and height of 20 mm (Fig. 1a). The six layers have the same geometry and dimensions, while they differ in the plate thickness. The frontal 2 layers; that are exposed to the blast pressure; have plate thickness of 0.4 mm. The inner two layers, have plate thickness of 0.8 mm while the rear two plates have plate thickness of 1.2 mm (Fig. 1b). Hence, the total thickness of the auxetic core is ~130 mm (including the thickness of the layers and 1 mm gap between them). The layers are made of AL6063-T4 aluminum material, a low strength aluminum commonly used in door, window, and furniture applications (yield point of 90 MPa). The selection of this particular grade was based on the findings of Al-Rifaie and Sumelka [8], which indicated that a weaker grade such as AL6063-T4 allows for more deformation in the core, greater energy absorption, and lower reaction forces in the supports [8].

In order to hold the corrugated core of the sandwich panel in place before and after blast pressure, a steel frame was required. The proposed steel frame is designed to be "easy to build" and serves as a substitute for the standard sandwich panel configuration, which consists of a frontal plate, corrugated core, and back steel plate, all of which are laser welded to keep them integrated. The dimensions, loading direction, and boundary conditions of the steel frame can be seen in the frontal (Figure 1c) and rear (Figure 1d) views. The overall dimensions of the steel frame are 330x330x150 mm, with a frontal clear opening of 300x300 mm that allows the blast pressure to impact the corrugated core (as shown in Figures 1c and e). The rear plate is reinforced with extra stiffeners of 16mm depth to reduce deflections due to the crushing impact of the corrugated core.

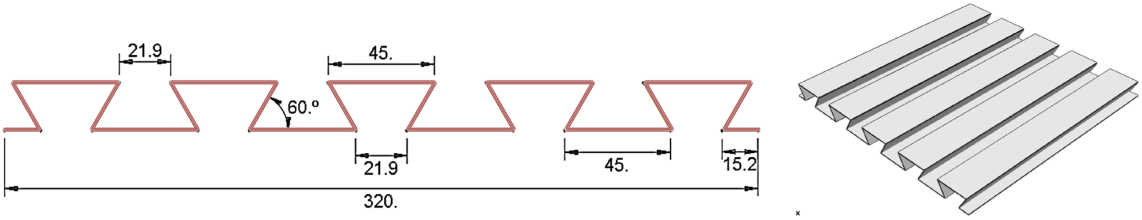

a) Cross-sectional dimensions (mm) and 3D view of one corrugated auxetic layer

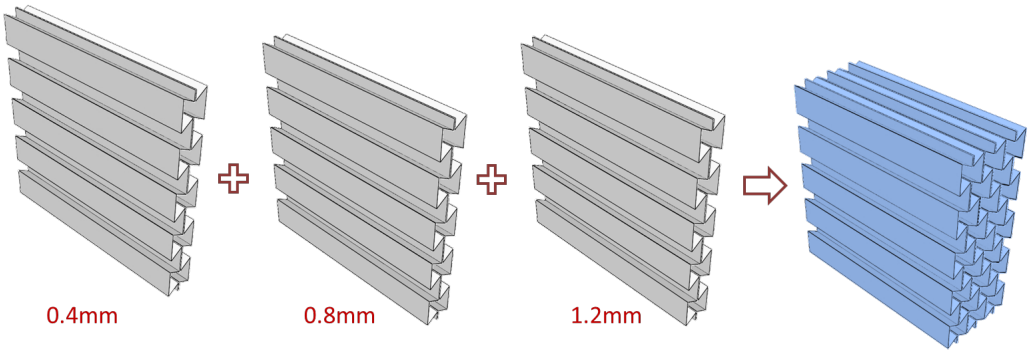

b) The plate thickness of the six layers composing the auxetic core

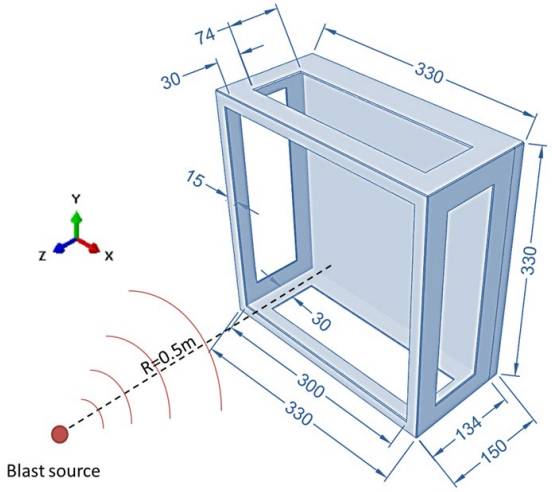

c) Frontal side of the steel frame [35]

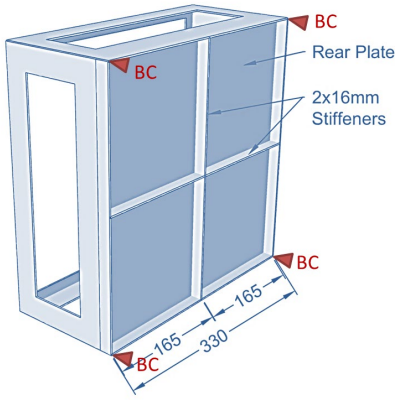

d) Rear side of the steel frame [35]

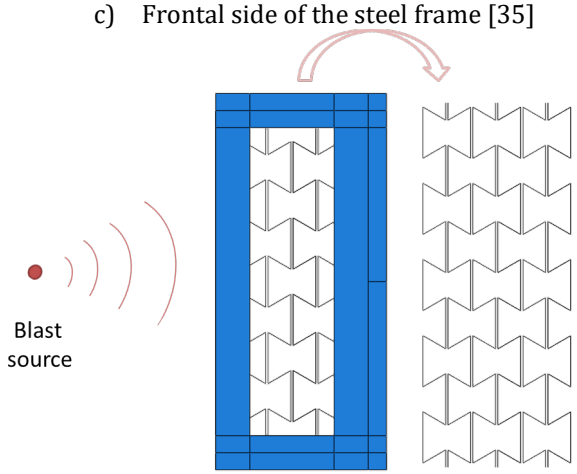

e) Side view of the sandwich panel and its core

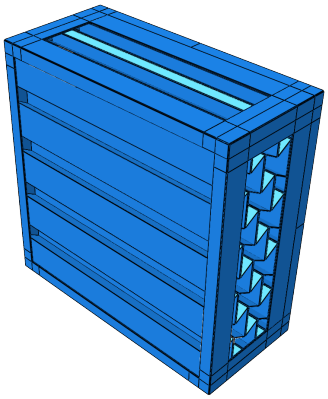

f) 3D view of the proposed sandwich panel

Figure 1. The geometry and dimensions of the proposed sandwich panel and its components

All the components of the steel frame have a unified material thickness of 2 mm, and the total mass of the steel frame is 4 kg. The inner space of the steel frame (330x330x134 mm) accommodates the core (320x320x130 mm) with a few millimetres gap on each side, allowing the layers to move freely within the frame's space without any connection between the layers or between the layers and the frame. The steel frame is made of Weldox 460E steel grade, which was chosen for its ductility and high strength.

3. Blast loading

The angle of incident, mass of explosive material (M), and stand-off distance (R) are the primary factors that need to be examined in blast pressure analysis. It has been established that peak reflected overpressure is achieved when the angle of incident is 0°, which is the angle between the wave propagation vector from the explosive centroid towards the target and the outward normal of the reflecting surface [40, 55]. Hence, for this study, the angle of incident is assumed to be 0°. The mass (M) of the Improvised Explosive Device (IED), which is the second factor, is provided in a range of TNT equivalency by the US Department of Homeland Security in the FEMA report [56], depending on the transport form such as luggage, a car or a van with a maximum carrying weight of 45 kg, 200 kg, or 2000 kg, respectively. Finally, the stand-off distance (R) needs to be greater than the longest dimension of the target to avoid localized effects and receive a relatively uniform blast pressure.

Table 1. The five blast intensities considered in this study, their scaled distances and the corresponding peak reflected overpressure time histories generated by ConWep [35].

Blast Intensities	Mass of TNT at R=0.5 m	Scaled distance Z $Z = \frac{R}{\sqrt[3]{M}}$ [m/ kg$^{\frac{1}{3}}$]
BI-1	M=0.1 kg	Z= 1.08
BI-2	M=0.2 kg	Z= 0.85
BI-3	M=0.3 kg	Z= 0.75
BI-4	M=0.4 kg	Z= 0.68
BI-5	M=0.5 kg	Z= 0.63

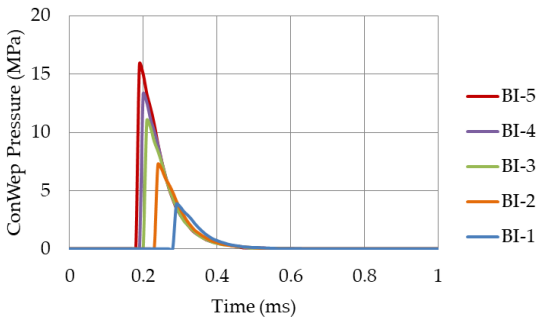

This paper examines five blast intensities, designated as BI-1 to BI-5, and their corresponding M-R combinations. Table 1 provides a list of these combinations, where the mass is measured in kg of TNT or its equivalent and the stand-off distance R is in meters. The scaled distance Z in m/kg$^{1/3}$, can be used to link the mass and stand-off distance. The chosen M-R combinations represent possible person-borne TNT, which are equivalent to TNT carried in luggage, car, or van with larger stand-off distances. Using the ConWep tool in Abaqus, the peak reflected overpressure time histories were calculated for the five blast intensities. The peak reflected overpressure values for BI-1 to BI-5 are 3.83, 7.25, 11.02, 13.29, and 15.86 MPa, respectively. The arrival time for the frontal shock wave varies by approximately 0.2 ms (Table 1).

4. Numerical Model

In this study, the sandwich panel was modelled using Abaqus (CAE) software and analyzed through the Abaqus (Explicit) numerical solver. To simulate the steel frame and the aluminium corrugated core, 3D deformable shell elements were employed, utilizing five points of integration within their thicknesses. For both materials, two homogeneous isotropic sections were defined. The elasto-plastic material model was used, which incorporates Johnson-Cook strain hardening and damage initiation. The Johnson-Cook material model is a constitutive model that can reproduce the plastic behavior of the material under high strain rates and high temperatures. Based on Johnson-Cook model, the yield stress σ_y in Eq. (1) considers strain rate hardening and thermal softening effects [57–60]:

$$\sigma_y = (A + B\,\varepsilon^n)\left[1 + C\,\ln(\frac{\dot{\varepsilon}}{\dot{\varepsilon_0}})\right]\left[1 - (\hat{T})^m\right] \quad (1)$$

where, ε is the plastic strain, $\dot{\varepsilon}$ is the plastic strain rate, $\dot{\varepsilon_0}$ is the reference plastic strain rate and $\hat{T}$ is the dimensionless temperature parameter that depends on the current material temperature, room temperature and melting point of the material.

The plastic strain at failure ε_f rely on non-dimensional plastic strain rate $\frac{\dot{\varepsilon}}{\dot{\varepsilon_0}}$, pressure to Mises stress ratio $\frac{p}{q}$, dimensionless temperature parameter $\hat{T}$ and $(d_1 - d_5)$ failure parameters as follow:

$$\varepsilon_f = \left[d_1 + d_2\exp(d_3\,\frac{p}{q})\right]\left[1 + d_4\,\ln(\frac{\dot{\varepsilon}}{\dot{\varepsilon_0}})\right](1 + d_5\,\hat{T}) \quad (2)$$

The sources of material parameters are Børvik, et al. [61] for Weldox 460E Steel and ASM Specification Aerospace Metals [62] for AL6063-T4 aluminium, and can be found in Table 2, as summarized in [35] based on the input requirements of Abaqus software.

Table 2. Johnson-Cook material model parameters for Weldox 460E Steel [61] and AL6063-T4 aluminium [62] used for the frame and the auxetic corrugated core, respectively.

Category	Constant	Description	Unit	Weldox 460E Steel	AL6063-T4
Elastic Constants	E	Modulus of Elasticity	GPa	200	68.9
	ν	Poisson's ratio	-	0.33	0.33
Density	ρ	Mass density	kg/m^3	7850	2703
Yield stress and strain hardening	A	Yield Strength	MPa	490	89.6
	B	Ultimate Strength	MPa	807	172
	n	work-hardening exponent	-	0.73	0.42
Strain-rate hardening	$\dot{\varepsilon_0}$	Reference Strain rate	s^{-1}	5*· 10^{-4}	1·10^{-4}
	C	strain rate factor	-	0.0114	0.002
Damage evolution	D_c	Critical Damage	-	0.3	0.3
	p_d	Damage threshold	-	0	0
Adiabatic heating and temperature softening	C_p	Specific heat	mm^2 · K/s^2	452·10^6	910·10^6
	χ	Taylor Quinney empirical constant/inelastic heat fraction	-	0.9	0.9
	T_m	Melting Temperature	K	1800	616
	T_0	Room Temperature	K	293	293.2
	m	thermal-softening exponent	-	0.94	1.34
Fracture Strain Constants	d_1	-	-	0.0705	-0.77
	d_2	-	-	1.732	1.45
	d_3	-	-	-0.54	0.47
	d_4	-	-	-0.015	0.00314
	d_5	-	-	0	1.6

The sandwich panel's length runs parallel to the x-axis, its height to the y-axis, and that the blast pressure and relative deformations occur along the z-axis (as seen in Figure 1c). To simulate the effects of plastic strains generating heat, the "Adiabatic heating effects" were included, assuming an inelastic heat fraction of $\chi = 0.9$. A non-linear dynamic explicit step was used for the simulation, with a total time of 0.01s (10ms). A general explicit contact was defined for the entire assembly, incorporating both tangential and normal contact options. The tangential behavior was implemented using a "penalty" friction formulation with a coefficient of friction of 0.3, while a "hard" contact was utilized for the normal behavior. As previously mentioned in Section 3, the ConWep software was employed for the blast loading with the "air blast" option. The proposed sandwich panel was assumed to be supported by four nodal boundary conditions (BC) at the corners, restraining the Z-direction and providing concentrated nodal reaction forces, while all other translational and rotational degrees of freedom were left free. This type of BC was chosen because it was deemed the most critical in terms of expected deformations and plastic strain in the sandwich panel.

For the steel frame and aluminum layers, a 4 node doubly curved shell (S4 elements) was selected. To determine the most cost-effective computational model with high accuracy, a mesh study was conducted checking three different mesh sizes: 2.5 mm, 5 mm, and 10 mm. Among these options, the 2.5 mm and 5 mm mesh sizes were chosen for the auxetic layers and the steel frame, respectively. The whole numerical model comprises 212940 finite elements and 1294092 degrees of freedom.

5. Results and Discussions

This section aims to find deformations, reaction forces and dissipation energy of the proposed auxetic sandwich panel and compare them with the non-auxetic trapezoidal topology presented in [35].

5.1 Deformations

As is widely understood, the deformation and crushworthiness of corrugated cores typically occur in three stages: elastic, plateau, and densification [63]. These stages can take place in a matter of milliseconds, with the elastic and densification stages being relatively short when compared to the plateau stage. During the plateau stage, which is the longest of the three stages, plastic deformations predominantly occur.

Table 3 displays the deformation of the corrugated cores for the five blast intensities studied, at selected representative time steps (0.5, 1 and 3 ms). Additionally, the table presents a 3D view of the panel with peak deformations. The last column shows the peak deformation value *d* (between 0-10 ms of the analysis), and the core compressive strain, *CS* (peak deformation divided by the total core thickness of 130 mm). It should be noted that the last two columns of Table 3 do not necessarily correspond to a specific time point, as this can vary depending on the blast intensity. The peak deformation value, *d*, was not measured at a pre-defined specific location of the core and was instead based on the Abaqus/Explicit output, primarily in the frontal layer of the core.

Looking at time steps 0.5-3 ms (Table 3), the auxetic cores reveal progressives collapse (layer by layer) with different pace based on the applied blast intensity. At 0.5ms, only the 1st frontal layer was compressed for BI-1 compared to the frontal 3 layers for BI-5. At time of 1ms, additional layers were deformed and the general response of the cores started to differ. At time 3ms, when peak deformations were almost achieved, the auxetic densification (with lateral shrinkage) is visible. The compressive strains are gradually increasing from 57% (for BI-1) to 94% (for BI-5). This shows the superior compatibility of the proposed sandwich panel to different blast intensities because the full densification was not reached (undesired case that can lead to sudden impact on the supports of a structure). It is important to notice that due to the high blast pressure of BI-5 (~16 MPa), damage occurred in the frontal layer causing elements to get seperated from the sandwich panel (as seen in the last row of Table 3). Regarding the steel frame, the material generally remained in the elastic zone, except towards the supporting corners, where small non-elastic deformations were noticed.

Table 3. The deformations d (in mm) and compressive strains (CS) of the corrugated auxetic cores when subjected to the five blast intensities considered in this study (Table 1).

Time [ms]	0.5	1	3	3D view	d (CS)
BI-1	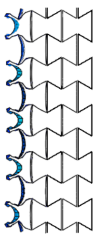	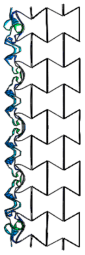	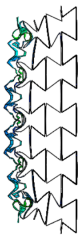	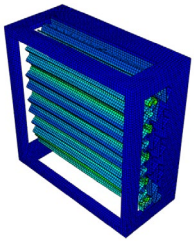	74mm (~0.57)
BI-2	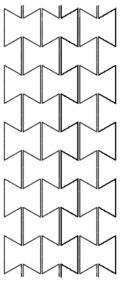	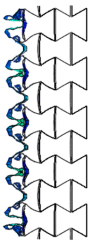	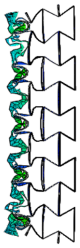	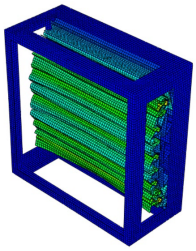	101mm (~0.78)
BI-3	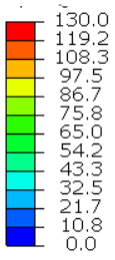	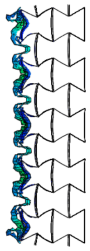		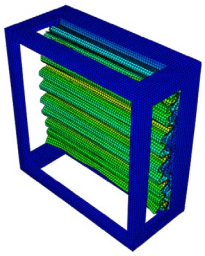	106mm (~0.82)
BI-4		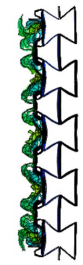		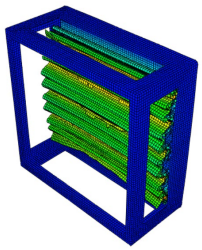	118mm (~0.91)
BI-5	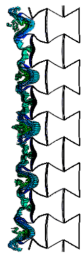	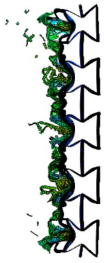		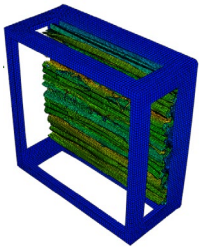	122 mm (~0.94)

5.2 Reaction forces

One of the most important aspects to consider when employing sandwich panels is the reaction forces. The unabsorbed blast energy is sent to the protected target to which the sacrificial panel is connected through boundary conditions/supports. The more energy absorbed by the core, the lower the predicted reaction forces. Figure 2a illustrates the influence of blast intensity on the time-history of nodal reaction force (in one support) while Figure 2b shows the peak values.

A monolithic solid plate was also simulated, and its reaction forces to blast intensity (BI-5) were measured. It was found that the peak nodal reaction forces of a solid plate can reach 44kN compared to only 20kN when adopting the suggested auxetic sandwich panels as energy absorbers. In other words, employing the proposed auxetic sandwich panel can decrease ~55% of the reaction forces, resulting in less loading on the target that has to be protected. These findings are in line with the findings of [40], which found that 49% of peak reaction forces can be reduced.

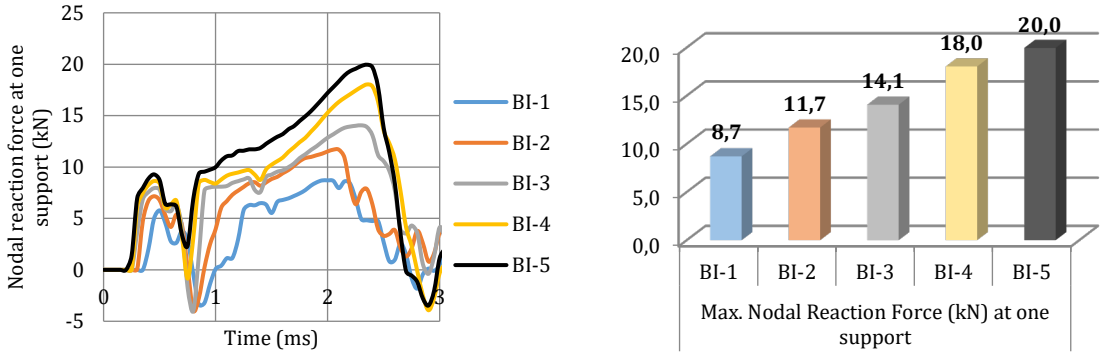

(a) Nodal reaction force time-history **(b)** Maximum nodal reaction force

Figure 2. The nodal reaction force of the proposed sandwich panel (in one corner of the four BC presented in Figure 1d), when subjected to the five different blast intensities considered in this study (Table 1).

5.3 Energy Dissipation

The plastic dissipation energy (PDE) of the entire numerical model (frame+core) is the most significant aspect to evaluate since the goal of this study is the development of a novel efficient blast-absorbing sacrificial sandwich panel. The PDE of the graded auxetic sandwich panel proposed here is compared to the trapezoidal graded sandwich panel presented in [35], where their results clearly show that the trapezoidal topology is the most efficient option when compared to other non-auxetic topologies, with uniform compression, lower reaction forces, and higher PDE. Results (Figure 3) shows that the PDE of the graded auxetic topology is higher than that of the trapezoidal topology. This is linked to the auxetic lateral shrinkage, which condenses the structure and causes increased plastic strain. The difference is increasing gradually with increasing the blast intensity up to 3 kJ for BI-5 (10 kJ for the trapezoidal topology compared to 13 kJ for the re-entrant auxetic topology).

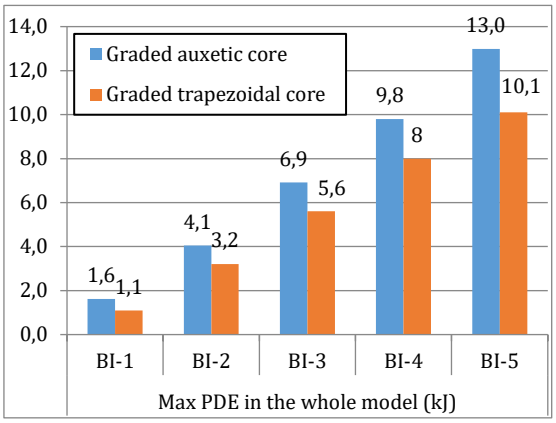

Figure 3. Plastic Dissipation Energy of auxetic (presented here) and trapezoidal (presented in [35]) sandwich panels for blast intensities BI-1 to BI-5.

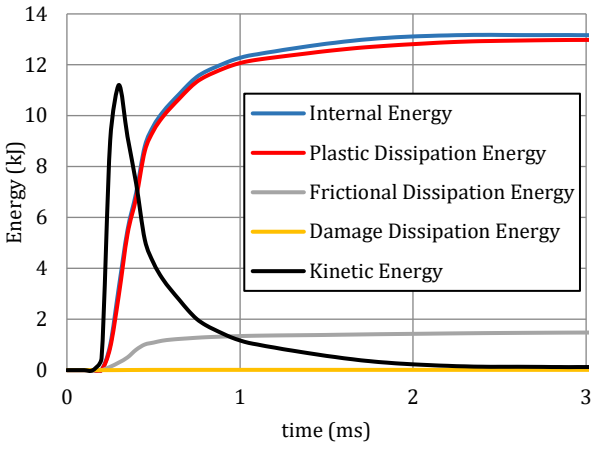

Figure 4. Energy components of the graded auxetic sandwich panel, when subjected to 0.5kg of TNT at R=0.5m (BI-5).

Furthermore, data (in Figure 4) demonstrate that the internal energy (IE) in the graded auxetic core is mostly constituted of Plastic Dissipation Energy (PDE), Frictional Dissipation Energy (FDE), and very minimal damage dissipation energy (DDE) as a result of visible damage in the frontal layers (Figure 5).

The black curve in Figure 4 represents the kinetic energy of the whole sandwich panel that drops to zero in 3 ms, revealing the excellent shock absorption potential of the proposed sandwich panel. The energy components (IE, PDE, FDE, and DDE) for the whole numerical model were recorded using Abaqus built-in history output requests.

Figure 5 shows the maximum equivalent plastic strain through the section points at integration points (abbreviated in Abaqus as PEEQMAX) of the auxetic sandwich panel, when subjected to 0.5kg of TNT at R=0.5m (BI-5). The first 2 layers were partially damaged with major plastic strain (Figure 5 c-d). The second 2 layers (Figure 5 e-f) showed major plastic strain with no visible damage. The last 2 layers (Figure 5 g-h) showed only minor plastic strain.

In short, the suggested sandwich panel outperforms other topologies and may be utilised to safeguard a wide range of blast-vulnerable structures, from multi-story buildings to armoured vehicles.

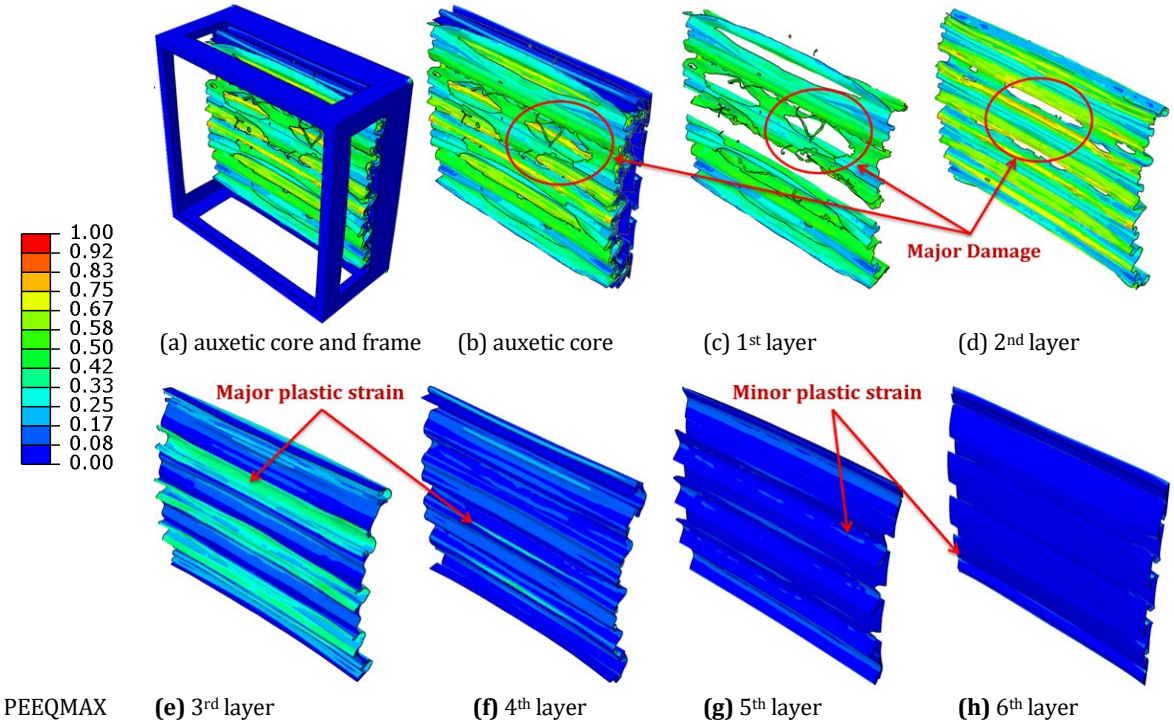

Figure 5. Maximum equivalent plastic strain through the section points at integration points (abbreviated in Abaqus as PEEQMAX) of the auxetic sandwich panel, when subjected to 0.5kg of TNT at R=0.5m (BI-5).

6. Conclusions

The objective of this computational study was to create a simple-to-assemble, low-cost graded sandwich panel that may be employed as a multi-purpose sacrificial defensive structure for a wide range of blast threats. The suggested auxetic sandwich panel is composed from detached corrugated aluminium layers that are placed in a steel frame.

The auxetic core revealed progressives collapsed at different rates depending on the applied blast intensity. The compressive strains increased gradually from 57% (for BI-1) to 94% (for BI-5). Because full densification was not achieved, this demonstrates the superior compatibility of the proposed sandwich panel to different blast intensities. Peak nodal reaction forces for BI-1 to BI-5 ranged from 8.7 to 20 kN. When compared to a monolithic plate, the proposed auxetic sandwich panel can reduce reaction forces by up to 55%, resulting in less loading on the target that must be protected. The plastic dissipation energy was higher than in equivalent non-auxetic topologies due to auxetic lateral shrinkage, which condenses the structure and causes increased plastic strain. The results also show that the internal energy in the graded auxetic core is primarily made up of plastic dissipation energy, frictional dissipation energy, and very little damage dissipation energy due to visible damage in the front two layers.

The sacrificial sandwich panel shown here can defend buildings' frontal façades, armoured vehicles, bridge piers, gates, and other vulnerable structures. The author's future interests include the manufacturing and field testing of the suggested sandwich panel.

Acknowledgments

Acknowledgment goes to Project no. 0411/SBAD/0006, Faculty of Civil and Transport Engineering, Poznan University of Technology.

Additional information

The author declare: no competing financial interests and that all material taken from other sources (including their own published works) is clearly cited and that appropriate permits are obtained.

References

1. H. Draganić, G. Gazić, D. Varevac; Experimental investigation of design and retrofit methods for blast load mitigation–A state-of-the-art review; Engineering Structures, 2019, 190, 189-209
2. P. Sielicki, T. Łodygowski, H. Al-Rifaie, W. Sumelka; Designing of Blast Resistant Lightweight Elevation System-Numerical Study; Procedia Engineering, 2017, 172, 991-998
3. S. A. Mazek; Performance of sandwich structure strengthened by pyramid cover under blast effect; Structural Engineering and Mechanics, 2014, 50, 471-486
4. S. Lotfi, S. M. Zahrai; Blast behavior of steel infill panels with various thickness and stiffener arrangement; Structural Engineering and Mechanics, 2018, 65, 587-600
5. H. Al-Rifaie, W. Sumelka; Numerical analysis of reaction forces in blast resistant gates; Structural Engineering and Mechanics, 2017, 63, 347-359
6. R. Alberdi, J. Przywara, K. Khandelwal; Performance evaluation of sandwich panel systems for blast mitigation; Engineering Structures, 2013, 56, 2119-2130
7. H. Al-Rifaie; Application of Passive Damping Systems in Blast Resistant Gates; I ed. Poznan, Poland: Wydawnictwo Politechniki Poznańskiej, 2019
8. H. Al-Rifaie, W. Sumelka; The developement of a new shock absorbing Uniaxial Graded Auxetic Damper (UGAD); Materials, 2019, 12, 2573
9. N. Novak, M. Vesenjak, Z. Ren; Auxetic cellular materials-a review; Strojniški vestnik-Journal of Mechanical Engineering, 2016, 62, 485-493
10. N. Novak, L. Starčevič, M. Vesenjak, Z. Ren; Blast response study of the sandwich composite panels with 3D chiral auxetic core; Composite Structures, 2019, 210, 167-178
11. P. Baranowski, J. Malachowski, L. Mazurkiewicz; Numerical and experimental testing of vehicle tyre under impulse loading conditions; International Journal of Mechanical Sciences, 2016, 106, 346-356
12. Z. Nowak, M. Nowak, R. Pecherski, M. Potoczek, R. Sliwa; Numerical simulations of mechanical properties of alumina foams based on computed tomography; Coupled Field Problems and Multiphase Materials, 2017, 107
13. E. Andrews, W. Sanders, L. J. Gibson; Compressive and tensile behaviour of aluminum foams; Materials Science and Engineering: A, 1999, 270, 113-124
14. R. B. Pecherski, M. Nowak, Z. Nowak; Virtual metallic foams. Application for dynamic crushing analysis; International Journal for Multiscale Computational Engineering, 2017, 15(5), 431-442
15. D. Papadopoulos, I. C. Konstantinidis, N. Papanastasiou, S. Skolianos, H. Lefakis, D. Tsipas; Mechanical properties of Al metal foams; Materials letters, 2004, 58, 2574-2578
16. L. Peroni, M. Avalle, M. Peroni; The mechanical behaviour of aluminium foam structures in different loading conditions; International Journal of Impact Engineering, 2008, 35, 644-658
17. L. J. Gibson, M. F. Ashby; Cellular solids: structure and properties: Cambridge University Press, 1999
18. K. P. Dharmasena, H. N. Wadley, Z. Xue, J. W. Hutchinson; Mechanical response of metallic honeycomb sandwich panel structures to high-intensity dynamic loading; International Journal of Impact Engineering, 2008, 35, 1063-1074
19. X. Li, P. Zhang, Z. Wang, G. Wu, L. Zhao; Dynamic behavior of aluminum honeycomb sandwich panels under air blast: Experiment and numerical analysis; Composite Structures, 2014, 108, 1001-1008
20. H. Rathbun, D. Radford, Z. Xue, M. He, J. Yang, V. Deshpande, et al.; Performance of metallic honeycomb-core sandwich beams under shock loading; International journal of solids and structures, 2006, 43, 1746-1763
21. L. Hu, T. Yu; Dynamic crushing strength of hexagonal honeycombs; International Journal of Impact Engineering, 2010, 37, 467-474
22. D. Okumura, N. Ohno, H. Noguchi; Post-buckling analysis of elastic honeycombs subject to in-plane biaxial compression; International Journal of Solids and Structures, 2002, 39, 3487-3503

23. Z. Zou, S. Reid, P. Tan, S. Li, J. Harrigan; Dynamic crushing of honeycombs and features of shock fronts; International Journal of Impact Engineering, 2009, 36, 165-176
24. D. Ruan, G. Lu, B. Wang, T. X. Yu; In-plane dynamic crushing of honeycombs—a finite element study; International Journal of Impact Engineering, 2003, 28, 161-182
25. H. AL-RIFAIE, W. Sumelka; Auxetic Damping Systems for Blast Vulnerable Structures; in Handbook of Damage Mechanics, G. Z. Voyiadjis, Ed., II ed: Springer, 2020, 25
26. S. Xu, J. H. Beynon, D. Ruan, G. Lu; Experimental study of the out-of-plane dynamic compression of hexagonal honeycombs; Composite Structures, 2012, 94, 2326-2336
27. A. A. Nia, M. Sadeghi; The effects of foam filling on compressive response of hexagonal cell aluminum honeycombs under axial loading-experimental study; Materials & Design, 2010, 31, 1216-1230
28. P. Zhang, J. Liu, Y. Cheng, H. Hou, C. Wang, Y. Li; Dynamic response of metallic trapezoidal corrugated-core sandwich panels subjected to air blast loading–An experimental study; Materials & Design (1980-2015), 2015, 65, 221-230
29. C. J. Wiernicki, F. Liem, G. D. Woods, A. J. Furio; Structural analysis methods for lightweight metallic corrugated core sandwich panels subjected to blast loads; Naval Engineers Journal, 1991, 103, 192-202
30. R. Studziński, T. Gajewski, M. Malendowski, W. Sumelka, H. Al-Rifaie, P. Peksa, et al.; Blast test and failure mechanisms of soft-core sandwich panels for storage halls applications; Materials, 2021, 12, 70
31. H. Al-Rifaie, P. Wożniak, T. Łodygowski; Improving the blast resistance of steel columns using trapezoidal sandwich panels; in Science for Defence: Safety for Critical Infrastructure, 1 ed Warsaw: Wydawnictwo Instytutu Technicznego Wojsk Lotniczych, 2022, 33-54
32. H. Al-Rifaie, R. Studziński, T. Gajewski, M. Malendowski, P. Peksa, W. Sumelka, et al.; Full scale field testing of trapezoidal core sandwich panels subjected to adjacent and contact detonations; in Modern Trends in Research on Steel, Aluminium and Composite Structures, ed: Routledge, 2021, 393-399
33. R. Studziński, Z. Pozorski; Experimental and numerical analysis of sandwich panels with hybrid core; Journal of Sandwich Structures & Materials, 2018, 20, 271-286
34. Y. Rong, J. Liu, W. Luo, W. He; Effects of geometric configurations of corrugated cores on the local impact and planar compression of sandwich panels; Composites Part B: Engineering, 2018, 152, 324-335
35. H. Al-Rifaie, R. Studziński, T. Gajewski, M. Malendowski, W. Sumelka, P. W. Sielicki; A new blast absorbing sandwich panel with unconnected corrugated layers—numerical study; Energies, 2021, 14(1), 214
36. X. Hou, Z. Deng, K. Zhang; Dynamic Crushing Strength Analysis of Auxetic Honeycombs; Acta Mechanica Solida Sinica, 2016, 29, 490-501
37. G. Imbalzano, S. Linforth, T. D. Ngo, P. V. S. Lee, P. Tran; Blast resistance of auxetic and honeycomb sandwich panels: Comparisons and parametric designs; Composite Structures, 2018, 183, 242-261
38. H. Al-Rifaie, N. Novak, M. Vesenjak, Z. Ren, W. Sumelka; Fabrication and Mechanical Testing of the Uniaxial Graded Auxetic Damper; Materials, 2022, 15, 387
39. N. Novak, H. Al-Rifaie, A. Airoldi, L. Krstulović-Opara, T. Łodygowski, Z. Ren, et al.; Quasi-static and impact behaviour of foam-filled graded auxetic panel; International Journal of Impact Engineering, 2023, 104606
40. H. Al-Rifaie, W. Sumelka; Improving the Blast Resistance of Large Steel Gates-Numerical Study; Materials, 2020, 13, 2121
41. A. Yeganeh-Haeri, D. J. Weidner, J. B. Parise; Elasticity of or-cristobalitez A silicon dioxide with a negative Poisson's ratio; Science, 1992, 257, 31
42. X. Y. Zhang, X. Ren, Y. Zhang, Y. M. Xie; A novel auxetic metamaterial with enhanced mechanical properties and tunable auxeticity; Thin-Walled Structures, 2022, 174, 109162
43. M. Zhang, H. Hu, H. Kamrul, S. Zhao, Y. Chang, M. Ho, et al.; Three-dimensional composites with nearly isotropic negative Poisson's ratio by random inclusions: Experiments and finite element simulation; Composites Science and Technology, 2022, 218, 109195
44. H. Al-Rifaie, W. Sumelka; Tłumik jednoosiowy dla układów bezpieczeństwa bram, drzwi lub okien (in Polish); Uniaxial damper as a safety system for gates, doors or windows. Patent, 2021,
45. J. Michalski, T. Strek; Blast resistance of sandwich plate with auxetic anti-tetrachiral core; Vibrations in Physical Systems, 2020, 31, 2020317
46. A. Mrozek, T. Strek; Numerical analysis of dynamic properties of an auxetic structure with rotating squares with holes; Materials, 2022, 15, 8712
47. J. Michalski, T. Strek; Response of a sandwich plate with auxetic anti-tetrachiral core to puncture; In: Advances in Manufacturing III. MANUFACTURING 2022. Lecture Notes in Mechanical Engineering; B. Gapiński, O. Ciszak, V. Ivanov (eds), Springer, Cham, 2022, 1-14.

48. T. Strek, J. Michalski, H. Jopek; Computational analysis of the mechanical impedance of the sandwich beam with auxetic metal foam core; Physica Status Solidi (b), 2019, 256, 1800423
49. A. Alderson; A triumph of lateral thought; Chemistry & Industry, 1999, 17, 384-391
50. W. Yang, Z.-M. Li, W. Shi, B.-H. Xie, M.-B. Yang; Review on auxetic materials; Journal of Materials Science, 2004, 39, 3269-3279
51. G. N. Greaves; Poisson's ratio over two centuries: challenging hypotheses; Notes Rec. R. Soc., 2013, 67, 37-58
52. Y. Liu, H. Hu; A review on auxetic structures and polymeric materials; Scientific Research and Essays, 2010, 5, 1052-1063
53. Y. Prawoto; Seeing auxetic materials from the mechanics point of view: a structural review on the negative Poisson's ratio; Computational Materials Science, 2012, 58, 140-153
54. H. Al-Rifaie, R. Studziński, W. Sumelka; A New Shock Absorbing Sandwich Panel with Unconnected Trapezoidal Corrugated Layers;presented at the Seventh International Symposium On Explosion, Shock Wave And High-strain-rate Phenomena, Maribor, Slovenia, 2023
55. S. E. Rigby, S. D. Fay, A. Tyas, J. A. Warren, S. D. Clarke; Angle of incidence effects on far-field positive and negative phase blast parameters; International Journal of Protective Structures, 2015, 6, 23-42
56. M. Chipley, W. Lyon, R. Smilowitz, P. Williams, C. Arnold, W. Blewett, et al.; Primer to Design Safe School Projects in Case of Terrorist Attacks and School Shootings. Buildings and Infrastructure Protection Series. FEMA-428/BIPS-07/January 2012. Edition 2; US Department of Homeland Security, 2012
57. G. R. Johnson, W. H. Cook; A constitutive model and data for metals subjected to large strains, high strain rates and high temperatures; in Proceedings of the 7th International Symposium on Ballistics, 1983, 541-547
58. G. R. Johnson, W. H. Cook; Fracture characteristics of three metals subjected to various strains, strain rates, temperatures and pressures; Engineering fracture mechanics, 1985, 21, 31-48
59. M. Grazka, J. Janiszewski; Identification of Johnson-Cook Equation Constants using Finite Element Method; Engineering Transactions, 2012, 60, 215–223
60. A. Shrot, M. Bäker; Determination of Johnson–Cook parameters from machining simulations; Computational Materials Science, 2012, 52, 298-304
61. T. Børvik, O. Hopperstad, T. Berstad, M. Langseth; A computational model of viscoplasticity and ductile damage for impact and penetration; European Journal of Mechanics-A/Solids, 2001, 20, 685-712
62. ASM Specification Aerospace Metals. Aluminum 6063-T4; Available: http://asm.matweb.com
63. S. Hou, C. Shu, S. Zhao, T. Liu, X. Han, Q. Li; Experimental and numerical studies on multi-layered corrugated sandwich panels under crushing loading; Composite Structures, 2015, 126, 371-385